AIAA JOURNAL
Vol. 45, No. 11, November 2007

Effects of Forced Asymmetric Transition on Vortex Asymmetry Around Slender Bodies

Bao-Feng Ma,* Xue-Ying Deng,† and Ying Chen‡
Beijing University of Aeronautics and Astronautics, 100083 Beijing, People's Republic of China

DOI: 10.2514/1.29712

A wind-tunnel experiment was conducted to study the effects of forced asymmetric transition on the asymmetric vortex system of a slender body by adding a grit strip on either side of the body. The results showed that the effect is very different depending on whether transition of the boundary layer occurs first on the higher vortex side or on the lower vortex side. If the transition first occurs on the higher vortex side, the transition will strongly influence the asymmetric vortex behavior and the side forces induced. The asymmetric vortex system will abruptly reverse its orientation when transition occurs and then gradually recover to its original position with increasing Reynolds number. However, if the transition first occurs on the lower vortex side, the trend of the asymmetric vortex system with increasing Reynolds number will be very similar to the case of natural transition. In addition, the asymmetric transition of the boundary layers on the forebody seems to have a dominant effect on the behavior of the asymmetric vortex system. The associated separation angles of the boundary layers appear to play a pronounced role in the development of the asymmetric vortex system.

Nomenclature

α	=	angle of attack
C_p	=	surface pressure coefficient, $(P - P_\infty)/(\frac{1}{2}\rho V_\infty^2)$
C_y	=	sectional side-force coefficients calculated by the integral of surface pressure
D	=	cylinder diameter
Re	=	Reynolds number based on the cylinder diameter, UD/v
X	=	axial coordinates
γ	=	roll angles, deg
θ	=	azimuth angles, deg
θs	=	separation angle (i.e., the minimum included angle between the separation point and the windward symmetry plane of a model), deg

I. Introduction

IT HAS long been known that slender bodies can produce asymmetric vortices at high angles of attack, even with no sideslip [1]. An asymmetric vortex could induce a time-averaged side force that is sometimes even larger than the normal force. The motivation for extensive studies in this subject mainly comes from the demand for enhanced maneuverability of modern aircraft and tactical missiles. However, the intrinsic fascination for the unique flow itself, in which axisymmetric bodies could produce asymmetric flow patterns, has also greatly motivated research interest.

Previous research [2–6] has revealed that a small imperfection on the nosetip could be responsible for the development of the asymmetric vortex. The tip imperfection, probably arising from manufacturing irregularities, could cause the experimental results obtained by various researchers on asymmetric vortices to show poor repeatability, because the imperfection distributions were different and random for the various models used, even for models with the same geometry. Therefore, Hunt [7] suggested that it was necessary to conduct a roll-angle sweep at the beginning of tests to identify roll angles in which the side forces are in a regular state and insensitive to the roll-angle changes, for the measurements to be repeatable from one model to another. This procedure has not yet been conclusively confirmed, but it appears to be a simple way of ensuring the repeatability of results in a bistable state. However, the experiments by Deng et al. [8] showed that an artificial tip perturbation could suppress the effect of any intrinsic natural imperfection on the nosetip and dominate the development of asymmetric vortices. By adding an artificial tip perturbation to the nosetip, repeatable results in terms of asymmetric vortex formation have been obtained in three wind tunnels with different turbulence levels and using two models manufactured differently but with the same geometry [8]. Moreover, this approach using an artificial tip perturbation ensured that the asymmetric vortex formation had a deterministic response to tip perturbation, because the information on the artificial perturbation, such as the position and size, was predetermined.

In addition to the nosetip, the Reynolds number is another key parameter that can have an important effect on asymmetric vortex formation over slender bodies [9–13]. After the transition of the boundary layer occurs, the change in the separation behavior due to the transition can significantly influence the asymmetric vortex system. Lamont [10,11] carried out a comprehensive test on an ogive cylinder in a pressurized wind tunnel over a wide range of Reynolds numbers. The results showed that the boundary layer exhibited laminar, transitional, and fully turbulent separation with increasing Reynolds number and that the side force induced would first gradually decrease and then rise up to the original value. In other words, the side force had larger values for laminar and fully turbulent separation, but in a transitional Reynolds number range, it remained smaller and almost approached zero. However, Ericsson and Reding [12] held a contrary viewpoint and suggested that the maximum side force should be produced in the transitional state, due to the asymmetric transition of the boundary layers. Hunt [7] and Lamont [11] argued that asymmetric transition could not influence the asymmetric vortices strongly enough for it to cause the maximum side force in a transitional Reynolds number range. They also believed, however, that asymmetric transition over slender bodies would probably exist. Recently, Deng et al. [13] found in experiments that not only does asymmetric transition exist, but that the transition also appears to always occur first on the lower vortex side. This finding seemed to indicate that the asymmetric transition is

Received 12 January 2007; revision received 4 June 2007; accepted for publication 7 June 2007.

*Postdoctoral Associate, Ministry-of-Education Key Laboratory of Fluid Mechanics; bf-ma@buaa.edu.cn.

†Professor, Ministry-of-Education Key Laboratory of Fluid Mechanics; dengxueying@vip.sina.com. Senior Member AIAA.

‡Ph.D. Candidate, Ministry-of-Education Key Laboratory of Fluid Mechanics; chenying@ase.buaa.edu.cn.

intrinsic to the nature of the asymmetric flow itself and that the flow itself could produce asymmetric transition even with uniform surface roughness. However, to date, no experiments have been performed to confirm whether or not transition must first occur on the lower vortex side or to examine how the asymmetric vortex formation and induced side forces would behave if the transition first occurred on the higher vortex side. In fact, it is possible that transition could occur first on the higher vortex side as a result of the nature of the flow itself or because of a nonuniform distribution of surface roughness on a model. Therefore, to further investigate the effect of asymmetric transition in detail, an artificial transition strip was used to induce asymmetric transition. The transition strip could be placed on either side of the slender body to allow transition to be initiated first on either the higher or the lower vortex side, as required. The forced asymmetric transition could be considered to be analogous to the behavior that may be produced over slender bodies with nonuniform surface roughness.

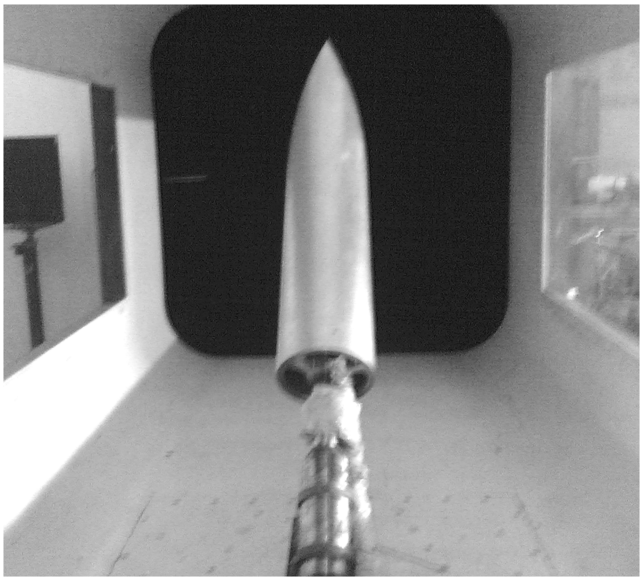

Fig. 1 Model installed in a wind tunnel.

II. Experimental Setup

The experiments were conducted in the D4 wind tunnel of the Institute of Fluid Mechanics of the Beijing University of Aeronautics and Astronautics. The wind tunnel is a low-speed, low-noise, and closed-return tunnel that can be run with either an open or closed test section. The interchangeable test sections are 1.5 m wide, 1.5 m high, and 2.5 m long, with a turbulence level of less than 0.1%. In the experiments, the closed test section was employed with a maximum freestream speed of up to 80 m/s. The model was sting-mounted and a motor behind the sting could drive the whole model to roll, as shown in Fig. 1. The model blockage at a 40-deg angle of attack was 5.7%.

The experimental model was a pointed ogive-tangent cylinder with a fineness ratio of 6D, as shown in Fig. 2a, and a cylinder diameter D of 200 mm. The model was arranged with 18 pressure measurement stations, and each station contained 24 equally spaced pressure taps. The internal pneumatic tubing made from stainless steel was connected to a PSI 9816 intelligent pressure Scanivalve system through soft rubber tubes with a 0.8-mm inner diameter. The pressure ranges of the PSI 9816 modules were all ± 1 psi (7 kPa).

A microtriangle block as an artificial tip perturbation was added onto the nosetip of the model to suppress the natural imperfection of the tip and to ensure the determinacy of the asymmetric vortex, as shown in Fig. 2b. All dimensions are in millimeters. The initial position of the perturbation was a 0-deg roll angle ($\theta = 0$ deg) that would rotate around the body axis with the rolling of the model.

The sketch of the grip-strip layout is shown in Figs. 3a and 3b. The grit strip was placed on either the lower or the higher vortex side, and the azimuth angle was 52.5 deg around the body from the windward symmetry plane. Regardless of whether it was placed on the lower or the higher vortex side, the grit strips were all divided into two parts. One was called a fore grit strip, which was located on the pointed-ogive part, but 50-mm away from the tip to avoid affecting the tip perturbation; the other was called an aft grit strip, which was located on the cylinder part. All grit strips were 7 mm wide, 0.3 mm thick, and used no. 80 microbeads with a 0.2-mm diameter. This grip-strip technique was implemented by Hall and Banks [14] to promote the transition of boundary layers over slender bodies at a high angle of attack by adding the grit strips on two sides of the body. In the present experiment, it was used to investigate the effect of forced asymmetric transition.

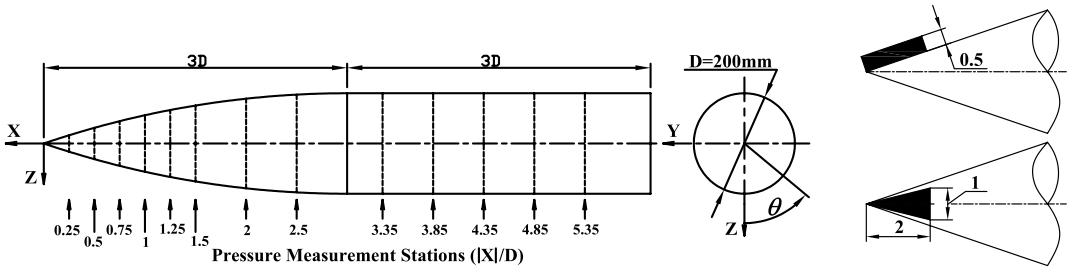

a) Ogive-cylinder model **b) Tip perturbation**

Fig. 2 Experimental model.

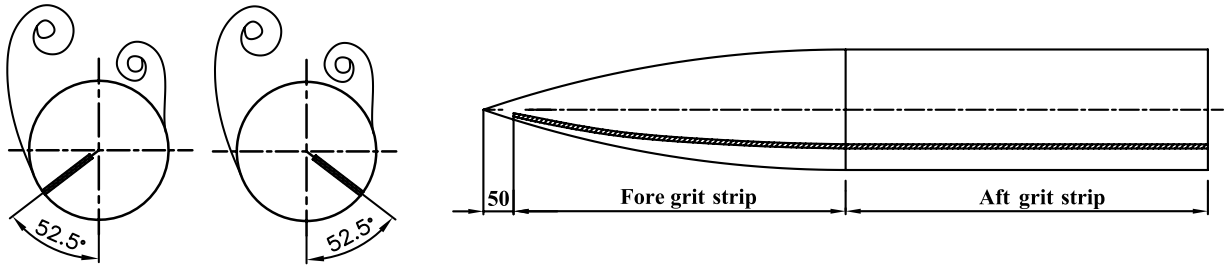

a) Grit strip on higher and lower vortex sides **b) Fore and aft grit strips**

Fig. 3 Grit-strip layout.

The model was fixed at a 40-deg angle of attack during the experiments. The freestream speed was varied from 5 to 70 m/s, and the corresponding Reynolds number based on the cylinder diameter ($D = 200$ mm) was in the range of 0.07 to 1.00×10^6 (the kinematic viscosity coefficient $\nu = 1.39 \times 10^{-5}$, determined by the freestream temperature). All experimental results were obtained by pressure measurement, and the sectional side-force coefficients were calculated by the integral of the surface pressure. The sampling rate of the Scanivalve system was set to 10 Hz and the number of averages was 100. The results provided in the following sections have been proven repeatable. The pressure measurements were repeated seven times at $\alpha = 40$ deg, $\gamma = 45$ deg, and $Re = 0.58 \times 10^{-6}$, and the corresponding rms error calculated was 0.0058 for the pressure coefficients at $|X|/\mathrm{D} = 4.35$ and 0.005 for the sectional side-force coefficient at $|X|/\mathrm{D} = 4.35$.

III. Results

A. Natural Transition

The asymmetric vortex around slender bodies can be influenced significantly by rolling the model, or even by rolling only the nosetip, and so the test for identifying the roll-angle effect should be conducted at the beginning of the experiments. By rolling the whole model, the variations of the sectional side forces with roll angles under a natural condition (without grit strips) were obtained, as shown in Fig. 4a. The curves exhibited classical double-cycle patterns: that is, the side forces changed four times with one rotation of the model. The four roll angles at 30, 120, 240, and 315 deg were selected to investigate the effect of forced asymmetric transition, as illustrated by the arrows in Fig. 4a, because it is at these roll angles that the asymmetric vortex system was fully developed and the side force induced was large.

The sectional side forces were also significantly dependent on the Reynolds numbers, especially the ones on the afterbody, as shown in Fig. 4b. They decreased first with increasing Reynolds numbers and even reversed their direction, and then rose up again when the Reynolds number was approximately more than 0.76×10^6. These results were consistent with Lamont's [10,11] findings . However, the freestream Reynolds numbers in Lamont's experiments were much larger (up to 4.0×10^6), due to the use of a pressurized wind tunnel, and so the side forces could continue to recover and finally attain the original direction and magnitude. In addition, Lamont found that for a model with a $2D$ nose fineness ratio, the sectional side forces only approached zero but did not reverse their direction, whereas for a model with a $3.5D$ nose fineness ratio, the direction was reversed [11]. Obviously, for the present model with a $3D$ nose fineness ratio, the behavior of the asymmetric vortex system over it is more similar to the latter.

B. Forced Asymmetric Transition

After adding a grit strip on either side of the body, the forced asymmetric transition would result in the asymmetric vortex system producing several changes compared with the case with natural transition. However, the experimental results showed that the changes were very different depending on whether the grit strip was on the higher vortex side or on the lower vortex side.

For the grit strip on the higher vortex side, the variation of the sectional side forces with Reynolds numbers were influenced significantly when the transition began to occur, as shown in Fig. 5. The sectional side forces exhibited a sharp drop around a Reynolds number of 0.18×10^6 and even became negative at the afterbody. They then gradually returned to the original positive values with increasing Reynolds number, as shown in Fig. 5a. The sharp drop can be seen more clearly in Fig. 5b, in which the side forces for the no-grip-strip and the fore-grip-strip-only cases are also presented. The general trend of the side force with increasing Reynolds number for the grip-strip cases was similar to the case under the condition of natural transition, but the decrease and reversal were greatly accelerated. More interestingly, the trend of C_y versus Reynolds number was almost identical for the two grip-strip cases.

A procedure for identifying the boundary-layer state in terms of time-averaged pressure distributions was used by Roshko [15] and followed by Lamont [10,11]. Based on pressure distributions, Roshko [15] divided the boundary-layer state around a

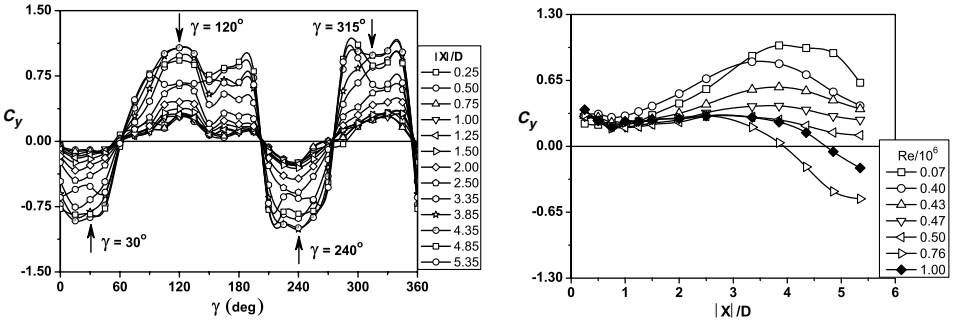

a) Roll angle effect, Re=0.14×10^6 b) Reynolds number effect, γ = 120 deg

Fig. 4 Variation of the sectional side forces without grit strips; $\alpha = 40$ deg.

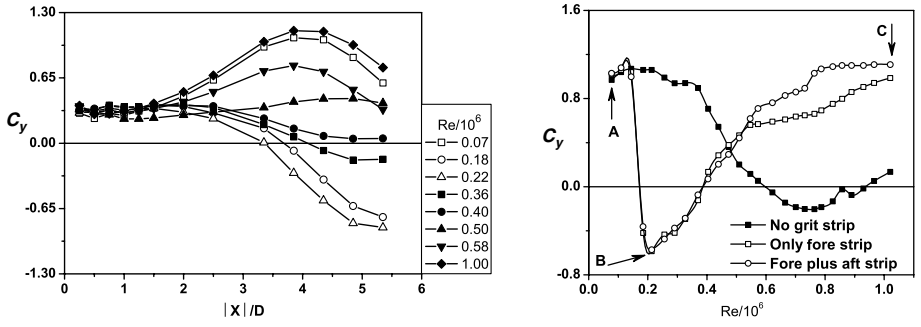

a) With fore plus aft grit strip b) At |X|/D=4.35

Fig. 5 Variation of the sectional side forces with Reynolds numbers for the grit strip on the higher vortex side; $\alpha = 40$ deg and $\gamma = 120$ deg.

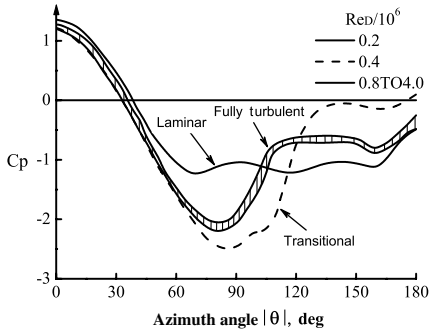

Fig. 6 Typical pressure distributions for different boundary-layer states, reproduced from Lamont [10].

two-dimensional cylinder by Reynolds numbers into three regimes: laminar, transitional, and fully turbulent. Lamont [10,11] had also, by this procedure, studied the variation of the separation types with Reynolds numbers over a three-dimensional ogive cylinder and classified the asymmetric vortical flow into three broad categories with laminar, transitional, and fully turbulent separations. Correspondingly, the three typical pressure distributions are shown in Fig. 6. The present authors also followed this procedure to analyze the results from the pressure measurements. However, it was difficult to distinguish between transitional and fully turbulent separation based on the present pressure distributions and so, for simplicity, these were all classed as turbulent separation in the present work.

The sectional pressure distributions are presented in Fig. 7 to demonstrate the separation types of the boundary layer and the behavior of the asymmetric vortices after adding the grit strip on the side of the higher vortex. When the Reynolds number was low enough, the boundary layers on both sides of the slender body experienced laminar separation regardless of whether a grit strip was in place or not, as shown in Fig. 7a, which corresponds to point A in Fig. 5b. The figure also shows that the vortex is higher on the left-hand side and lower on the right-hand side. Moreover, the separation angle on the lower vortex side was 30 deg larger than on the higher vortex side. This indicates that the separation was asymmetric even though the boundary layers of both sides experienced laminar separation.

When transition on the higher vortex side occurred with increasing Reynolds number, the positions of the left- and right-side vortices were reversed: that is, the one on the left side became the lower vortex and the one on the right became the higher vortex, as shown in Fig. 7b, which corresponds to point B in Fig. 5b. This reversal of the asymmetric vortex system was very interesting, but even more interesting was that the reversal behavior also occurred when only the fore grit strip was used. For both the cases of the fore–aft grit strip and the fore grit strip alone, the separation angle on the lower vortex side (left side) was always larger than the one on the higher vortex side (right side). The boundary layers on the right side (the original lower vortex side) all exhibited laminar separation and the separation angles were all at 90 deg. The separation types on the left-hand side were, however, different. With the fore–aft grit strip, there was turbulent separation ($\theta s = 135$ deg), whereas with only the fore grit strip, there was laminar separation ($\theta s = 105$ deg). This phenomenon appears to indicate that the vortex reversal can be principally attributed to boundary-layer transition on the forebody rather than on the afterbody. However, the difference in the separation types had little effect on the sectional side force, as shown in Fig. 5b.

When the Reynolds numbers were high enough, the separation type on both sides of the slender body became turbulent, as shown in Fig. 7c, which corresponds to point C in Fig. 5b. The vortex positions on the left and right sides were again reversed and recovered to their original orientation. In this case, the separation angle on the right-hand side (lower vortex side) became larger than the one on the left-hand side (higher vortex side). In addition, the pressure profiles were almost the same as those obtained using both the fore grit strip and using the combined fore–aft grit strip. More interestingly, the pressure distributions in Fig. 7c closely resemble those for turbulent separation obtained by Lamont [10,11] in experiments in which the Reynolds number was more than 2.0×10^6.

For the grit strip on the lower vortex side, no sharp drop was exhibited by the side force, and the trend of the side force with increasing Reynolds number was roughly similar to the case without a grit strip, as shown in Fig. 7. The only difference was that the sectional side force became larger in the positive direction at low Reynolds numbers (near point B in Fig. 8b), but larger in the negative direction at high Reynolds numbers (near point C in Fig. 8b). Furthermore, for both the fore–aft strip and the fore grit strip alone, the trend in side force was almost identical.

The sectional pressure distributions are also presented in Fig. 9 for the grit strip on the lower vortex side. Similar to the case for the grit strip on the higher vortex side, at low Reynolds numbers, the boundary layers on both sides of the body exhibited laminar separation and the separation angles were also similar, as shown in Fig. 9a (point A in Fig. 8b). It should be noted that for the fore–aft grit strip, the boundary layer on the left-hand side (lower vortex side) seemed to have been affected by the local grit strip and began to become transitional. This effect was not, however, significant and the separation type remained laminar. With increasing Reynolds number, the boundary layer on the lower vortex side began to exhibit turbulent separation first. As a result, the separation angle was much delayed and a larger suction peak was also induced on the lower vortex side, as shown in Fig. 9b. In contrast, the boundary layer on the higher vortex side initially continued to exhibit laminar separation. Also, the asymmetric vortex system did not reverse direction at this Reynolds number. In fact, the asymmetry level was enlarged due to the transition on one side. When the Reynolds number was high enough (more than 0.6×10^6), a reversal of the asymmetric vortex system occurred, as shown in Fig. 9c, and the boundary layers on both sides experienced turbulent separation. Regardless of this, Figs. 9a–9c show that the separation angle on the lower vortex side was always larger than the one on the higher vortex side.

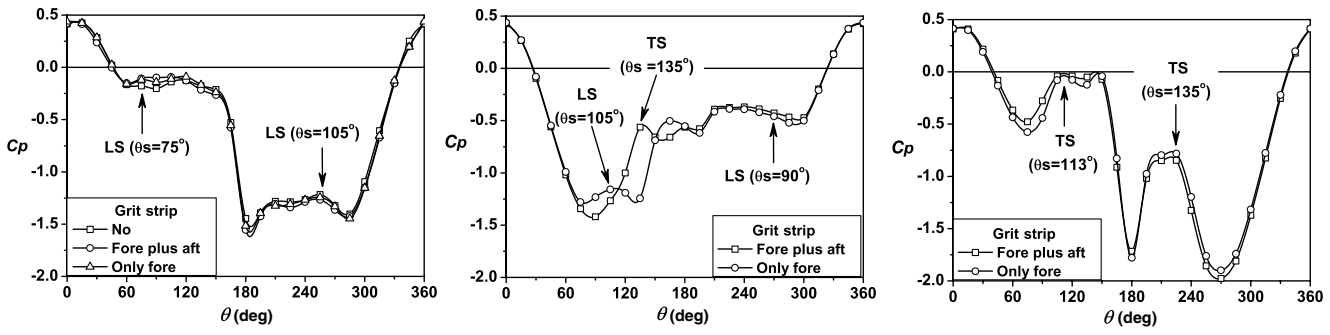

a) Re=0.07×10^6 **b) Re=0.22×10^6** **c) Re=1.00×10^6**

Fig. 7 Pressure distributions for the grit strip on the higher vortex side; $|X|/D = 4.35$, $\alpha = 40$ deg, and $\gamma = 120$ deg.

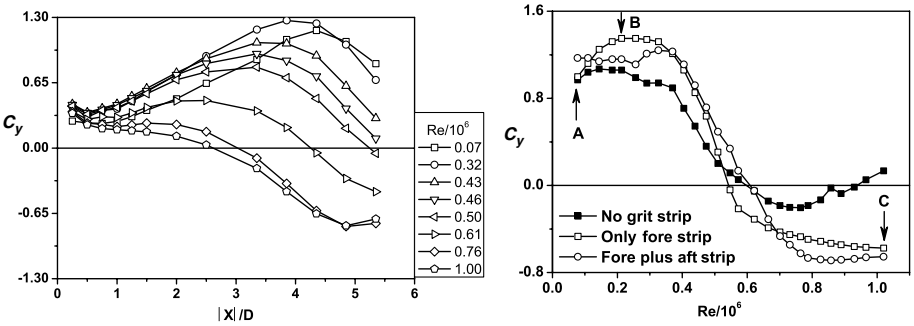

a) With fore plus aft grit strip b) At |X|/D=4.35

Fig. 8 Variation of the sectional side forces with Reynolds numbers for the grit strip on the lower vortex side; $\alpha = 40$ deg and $\gamma = 120$ deg.

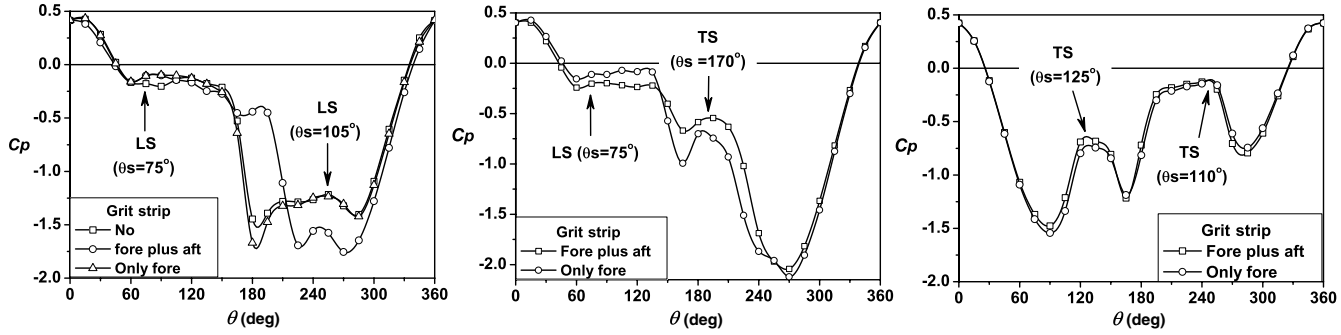

a) Re=0.07×10^6 b) Re=0.22×10^6 c) Re=1.00×10^6

Fig. 9 Pressure distributions for the grit strip on the lower vortex side; $|X|/D = 4.35$, $\alpha = 40$ deg, and $\gamma = 120$ deg.

IV. Discussion

A. Effects of Asymmetric Transition on the Asymmetric Vortex System

The investigation attempted to determine the effect of asymmetric transition on the asymmetric vortex behavior. The results show that asymmetric vortex behavior when transition occurred first in the boundary layer on the higher vortex side was very different from when it occurred first on the lower vortex side. If transition first occurred on the higher vortex side, the asymmetric vortex system at the afterbody would abruptly reverse its direction. However, if transition first occurred on the lower vortex side, the behavior of the asymmetric vortex system would be similar to the case for natural transition.

The local pressure distributions could provide information about the separation types of the boundary layers, as suggested by Roshkol [15] and Lamont [10], and so the reasons for the changes in the asymmetric vortex system due to the asymmetric transition can be analyzed further. Figures 5 and 7 show that the separation angles on the lower vortex side are always larger than those on the higher vortex side. These findings seem to indicate that the separation behavior of the boundary layers plays an important role in the development of the asymmetric vortex system. It is known that boundary layers after transition have a much better ability for pressure recovery and can resist the adverse pressure gradient better. As a result, the larger suction peak can be produced ahead of separation and, at the same time, the separation angle is delayed. The use of a grit strip on the forebody part has a particularly large effect on the vortex reversal. When adding the grit strip on the higher vortex side, boundary-layer transition on the forebody would cause the separation angle on the higher vortex side to be delayed, and consequently, the original higher vortex on that side would be pulled downwards. The vortex on the other side would then rise up. For the grit strip on the lower vortex side, the original large separation angle becomes even larger, and so the vortex position is not changed. However, it should be noted that the inversion of the side force only occurs on the afterbody and not on the forebody. This may be because the reversal of the asymmetric vortices is a gradual process from the forebody to the afterbody.

The results indicate that the surface roughness distribution is important for the behavior of the asymmetric vortex system. In particular, if the higher vortex side over a model has a higher surface roughness than the lower vortex side, then the experimental results would be influenced seriously when transition occurs.

Finally, additional flow visualizations appear to be necessary to confirm the vortex structure after the asymmetric transition occurs. However, traditional approaches to flow visualization, such as a smoke-flow method, make it difficult to obtain clear pictures at very high freestream speeds. The particle image velocimetry method is a feasible technique for future investigation of these phenomena.

B. Mechanism of Asymmetric Vortex Formation

In previous studies, two mechanisms were proposed to explain the development of the asymmetric vortex system. One mechanism, spatial instability, was suggested as the cause of the asymmetry. The other proposal, by Ericcson and Reding [12], suggested that the asymmetric separation of the boundary layers on the two sides of the slender body plays an important role during the formation of the asymmetric vortex system. Many previous studies [2,16–18] have proven that a little perturbation to the flow around the nosetip could amplify going downstream and trigger the asymmetric flow. This spatial convective instability would be responsible for the asymmetric vortex. The present findings indicate that this second mechanism is also very important for the development of the asymmetric vortex system.

In fact, the second mechanism does not seem to contradict the first one. Asymmetric separation is probably one of the principle factors that causes the flow instability over slender bodies, because if the separation angle is symmetrically fixed, then no asymmetric vortex would be produced, such as in the case of the vortical flow over a high-sweep delta wing, in which the separation points are fixed at the sharp leading-edges [19,20]. The asymmetric vortex is usually associated with asymmetric separation, and both seem to always coexist [21]. The previous and present results all revealed this point. At low Reynolds numbers (laminar separation), the separation angle on the higher vortex side is always smaller than the one on the lower vortex side. If this condition is modified, the asymmetric vortex

system would be affected significantly and could even reverse its orientation, as presented earlier. Therefore, asymmetric separation should be a necessary condition for the formation of the asymmetric vortex system.

V. Conclusions

The effects of asymmetric transition on asymmetric vortices were investigated by the addition of grit strips on a slender body. The following conclusions can be drawn:

If transition first occurs on the higher vortex side, the asymmetric transition would strongly influence the behavior of the asymmetric vortex system and the side force. The sectional side force would sharply decrease and even alter sign on the afterbody when transition occurs. Then with increasing Reynolds number, it would gradually recover to its original magnitude and sign again. This change in the side-force sign is attributed to the reversal of the asymmetric vortex system.

However, if transition first occurs on the lower vortex side, the asymmetric vortex behavior and the side force induced with Reynolds numbers is much more similar to the case for natural transition.

Boundary-layer transition on the forebody seems to have a dominant effect on the variation of the asymmetric vortex system with changing Reynolds number.

Boundary-layer transition influences the asymmetric vortex system mainly through altering the separation type of the boundary layer. In addition, the asymmetric separation of boundary layers plays an important role in the formation of the asymmetric vortex system. The separation angle on the higher vortex side is always smaller than the one on the lower vortex side, and if this condition were altered, the asymmetric vortex system would reverse its orientation.

Acknowledgments

The project is supported by the National Natural Science Foundation of China (10432020), the China Postdoctoral Science Foundation (20060390397), and the National Defense Foundation of China (9140A13020106HK0111).

References

[1] Thomson, K. D., and Morrison, D. F., "The Spacing, Position and Strength of Vortices in the Wake of Slender Cylinder Bodies at Large Incidence," *Journal of Fluid Mechanics*, Vol. 50, No. 4, 1971, pp. 751–783.

[2] Degani, D., and Tobak, M., "Experimental Study of Controlled Tip Disturbance Effect on Flow Asymmetry," *Physics of Fluids*, Vol. 4, No. 12, 1992, pp. 2825–2832.

[3] Bridges, D. H., and Hornung, H. G., "Elliptic Tip Effects on The Vortex Wake of an Axisymmetric Body at Incidence.," *AIAA Journal*, Vol. 32, No. 7, 1994, pp. 1437–1445.

[4] Luo, S. C., Lim, T. T., Lua, K. B., Chia, H. T., Goh, E. K. R., and Ho, Q. W., "Flowfield Around Ogive/Elliptic-Tip Cylinder at High Angle of Attack," *AIAA Journal*, Vol. 36, No. 10, 1998, pp. 1778–1787.

[5] Lee, A. S., Luo, S. C., Lim, T. T., Lua, K. B., and Goh, E. K. R., "Side Force on an Ogive Cylinder: Effects of Control Devices," *AIAA Journal*, Vol. 38, No. 3, 2000, pp. 385–388.

[6] Chen, X. R., Deng, X. Y., Wang, Y., Liu, P. Q., and Gu, Z. F., "Influence of Nose Perturbations on Behaviors of Asymmetric Vortices over Slender Body," *Acta Mechanica Sinica*, Vol. 18, No. 6, 2002, pp. 581–593.

[7] Hunt, B. L., "Asymmetric Vortex Forces and Wakes on Slender Bodies," AIAA Paper 82-1336, Aug. 1982.

[8] Deng, X. Y., Wang, G., Chen, X. R., Wang, Y. K., Liu, P. Q., and Xi, Z. X., "A Physical Model of Asymmetric Vortices Flow Structure in Regular State over Slender Body at High Angle of Attack," *Science in China (Series E)*, Vol. 46, No. 6, 2003, pp. 561–573.

[9] Bernhardt, J. E., and Williams, D. R., "Effect of Reynolds Number on Vortex Asymmetry about Slender Bodies," *Physics of Fluids*, Vol. 5, No. 2, 1993, pp. 291–293.

[10] Lamont, P. J., "Pressures around an Inclined Ogive Cylinder with Laminar, Transitional, or Turbulent Separation," *AIAA Journal*, Vol. 20, No. 11, 1982, pp. 1492–1499.

[11] Lamont, P. J., "The Complex Asymmetric Flow over a 3.5D Ogive Nose and Cylindrical Afterbody at High Angles of Attack," AIAA Paper 82-0053, Jan. 1982.

[12] Ericsson, L. E., and Reding, J. P., "Vortex-Induced Asymmetric Loads in 2-D and 3-D Flows," AIAA Paper 80-0181, 1980.

[13] Deng, X. Y., Ma, B. F., Chen, Y., Bo, N., and Wang, Y. K., "Reynolds Number Effects on Asymmetric Vortex Behaviors Around Slender Bodies," *Proceedings of the 11th Colloquium on Separated Flow, Vortex and Flow Control*, China Aerodynamics Research Society, Beijing, Oct. 2006, pp. 108–114 (in Chinese).

[14] Hall, R. M., and Banks, D. W., "Progress in Developing Gritting Techniques for High Angles of Attack Flows," AIAA Paper 94-0169, Jan. 1994.

[15] Roshko, A., "Experiments on the Flow Past a Circular Cylinder at Very High Reynolds Number," *Journal of Fluid Mechanics*, Vol. 10, No. 3, 1961, pp. 345–356.

[16] Bernhardt, J. E., and Williams, D. R., "Proportional Control of Asymmetric Forebody Vortices," *AIAA Journal*, Vol. 36, No. 11, 1998, pp. 2087–2093.

[17] Cai, J. S., Luo, Sh. j., and Liu, F., "Stability of Symmetric and Asymmetric Vortices over Slender Conical Wing-Body Combinations," *AIAA Journal*, Vol. 44, No. 7, 2006, pp. 1601–1608.

[18] Bridges, D. H., "The Asymmetric Vortex Wake Problem - Asking the Right Question," *36th AIAA Fluid Dynamics Conference*, AIAA, Reston, VA, 2006, pp. 1737–1765.

[19] Lowson, M. V., and Ponton, A. J. C., "Symmetry Breaking in Vortex Flows on Conical Bodies," *AIAA Journal*, Vol. 30, No. 6, 1992, pp. 1576–1583.

[20] Stahl, W. H., Mahmood, M., and Asghar, A., "Experimental Investigations of the Vortex Flow on Delta Wings at High Incidence," *AIAA Journal*, Vol. 30, No. 4, 1992, pp. 1027–1032.

[21] Ericsson, L. E., and Reding, J. P., "Aerodynamic Effects of Asymmetric Vortex Shedding from Slender Bodies," AIAA Paper 85-1797, Aug. 1985.

F. Coton
Associate Editor